Interfacial Recognition by Bee Venom Phospholipase A_2: Insights into Nonelectrostatic Molecular Determinants by Charge Reversal Mutagenesis†

Farideh Ghomashchi,‡ Ying Lin,‡ Mark S. Hixon,‡ Bao-Zhu Yu,§ Robert Annand,‡ Mahendra K. Jain,*,§ and Michael H. Gelb*,‡

Departments of Chemistry and Biochemistry, University of Washington, Seattle, Washington 98195-1700, and Department of Chemistry and Biochemistry, University of Delaware, Newark, Delaware 19716

Received October 13, 1997; Revised Manuscript Received December 4, 1997

ABSTRACT: The basis for tight binding of bee venom phospholipase A_2 (bvPLA2) to anionic versus zwitterionic phospholipid interfaces is explored by charge reversal mutagenesis of basic residues (lysines/arginines to glutamates) on the putative membrane binding surface. Single-site mutants and, surprisingly, multisite mutants (2−5 of the 6 basic residues mutated) are fully functional on anionic vesicles. Mutants bind tightly to anionic vesicles, and active-site substrate and Ca^{2+} binding are not impaired. Multisite mutants undergo intervesicle exchange slightly faster than wild type, especially in the presence of salt. It is estimated that electrostatic contribution to interfacial binding is modest, perhaps 2−3 kcal/mol of the estimated 15 kcal/mol. Elution properties of bvPLA2 from HPLC columns containing solid phases of tightly packed monolayers of phosphocholine amphiphiles suggest that ionic effects provide a modest portion of the interfacial binding energy and that this contribution decreases as the number of cationic residues mutated is increased. These results are consistent with the observation that Gila monster venom PLA2 (Pa2), which is homologous to bvPLA2, has high activity on anionic vesicles despite the fact that it has only a single basic residue on its putative interfacial recognition face. Results with bvPLA2 mutants show that manoalogue and 12-*epi*-scalaradial inactivate bvPLA2 by modification of K94. Also, deletion of the large β-loop (residues 99−118) is without consequence for interfacial binding and catalysis of bvPLA2. All together, the preferential binding of bvPLA2 to anionic vesicles versus phosphatidylcholine vesicles is mainly due to factors other than electrostatics. Therefore hydrogen-bonding and hydrophobic interactions must provide a major portion of the interfacial binding energy, and this is consistent with recent spectroscopic studies.

The hydrolysis of the *sn*-2 ester of glycerophospholipids by phospholipase A_2 (PLA2)[1] necessarily occurs at the lipid−water interface because naturally occurring phospholipids have virtually no solubility in water as monomers. All PLA2s characterized to date (*4*−*6*) are water-soluble enzymes that must bind to organized interfaces for catalytic turnover (*7*−*11*). Fourteen-kilodalton PLA2s are secreted from a number of cell types and are found in animal venoms, pancreatic digestive fluids, and mammalian cells of the inflammatory system. As supported by X-ray structures (*12*, *13*), these PLA2s require Ca^{2+} as an essential active-site cofactor to promote binding of a single substrate molecule in the active site and for the chemical step of lipolysis but not for binding to the interface (*4*, *14*, *15*).

There seems to be a general consensus that the binding of secreted PLA2s to membranes has significant electrostatic and hydrophobic components (*16*−*18*). These enzymes bind several orders of magnitude more tightly to anionic vesicles and mixed-micelles compared to neutral interfaces (*19*−*21*). In fact, at low ionic strength, the binding of most, if not all, 14-kDa PLA2s to anionic vesicles is virtually irreversible such that the bound enzyme hydrolyzes all of the phospholipids in the outer layer of vesicles without desorption of enzyme into the aqueous phase (*9*, *22*, *23*); this highly processive interfacial catalysis is termed scooting. Tight binding of 14-kDa PLA2s to anionic interfaces makes sense when one considers that biological interfaces have anionic surface potential due to the presence of anionic phospholipids and bile salts. Increasing ionic strength apparently leads to weaker enzyme−membrane binding such that the enzyme now hops from vesicle to vesicle (*24*).

High-resolution crystal structures are available for several 14-kDa PLA2s (reviewed in ref *18*), and all of these

† This work was supported by Grant HL36235 and Research Career Development Award GM562 to M.H.G., Grant GM29703 to M.K.J., and postdoctoral fellowship GM15464 to R.R.A., all from the National Institutes of Health.

* To whom correspondence should be addressed.
‡ University of Washington.
§ University of Delaware.

[1] Abbreviations: bvPLA2, 16-kDa phospholipase A_2 from the venom of honeybees (*Apis mellifera*); dansyl-DHPE, *N*-dansyl-1,2-dihexadecyl-*sn*-glycero-3-phosphoethanolamine; Δ99−118, mutant bee venom phospholipase A_2 in which residues 99−118 have been deleted; diC_6-thioPC, 1,2-bishexanoylthio-*sn*-glycero-3-phosphocholine; diC_6thioPM, 1,2-bishexanoylthio-*sn*-glycero-3-phosphomethanol; DMPC and DMPM, 1,2-dimyristoyl-*sn*-glycero-3-phosphocholine and -phosphomethanol; DTPC and DTPM, 1,2-ditetradecyl-*sn*-glycero-3-phosphocholine and -phosphomethanol; E5, K14E/R23E/K85E/K94E/K133E mutant of bee venom phospholipase A_2; EGTA, ethylene glycol bis(β-aminoethyl ether)-*N*,*N*,*N*′,*N*′-tetraacetic acid; i-face, interfacial recognition face of phospholipase A_2; Pa2, Pa2 isozyme of Gila monster venom (*Heloderma suspectum*) phospholipase A_2; PLA2, 14−18 kDa secreted phospholipase A_2; WT, wild-type bee venom phospholipase A_2.

S0006-2960(97)02525-7 CCC: $15.00
Published on Web 04/23/1998

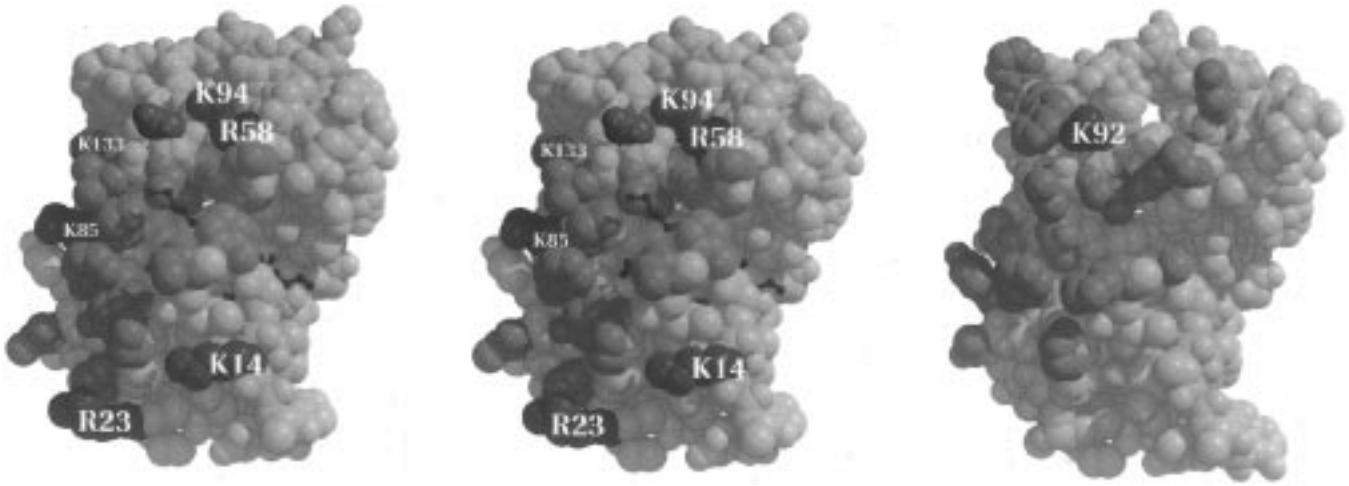

FIGURE 1: X-ray structure of bvPLA2 (left stereopair) and modeled structure of Pa2 (right). The orientation is with the viewer in the membrane looking out to the aqueous phase along a line perpendicular to the membrane plane (*52*). The short-chain phospholipid analogue seen in the X-ray structure of bvPLA2 (*18*) is shown in green. Residues on or near the putative i-face are color-coded as follows: lysines are shown in blue (14, 85, 94, and 133 for bvPLA2 and 92 for Pa5); arginines in are shown blue (23 and 58 for bvPLA2); acidic residues are shown in red (D92 for bvPLA2); hydrophobic residues are shown in purple (I1, Y3, P4, F24, I78, F82, M86, L90, and I91 for bvPLA2 and F1, P4, A11, Y53, Y54, P55, Y81, F82, V90, L91, F110, and W111 for Pa2); hydrophilic residues are shown in cyan (S11, H55, and H56 for bvPLA2 and T78, Q85, and T86 for Pa2); and segment 99−118 of bvPLA2 is shown in lime green.

structures contain cationic lysine and arginine residues on their putative interfacial recognition region (i-face) that surrounds the opening to the active-site slot. The secreted phospholipase A_2 from honeybee venom (bvPLA2) contains six cationic residues (K14, R23, R58, K85, K94, and K133) and a collection of hydrophobic residues that are potentially on the i-face of the protein, and the former could engage in electrostatic interactions with anionic phospholipids (Figure 1). D92 is the only anionic residues on this surface.

In this study, the consequences of changing the cationic i-face residues to anionic glutamate (charge reversal) has been explored in detail. Three related problems were also investigated: (1) All secreted PLA2s contain a β-loop of unknown function that lies off to one side of the active-site slot. For bvPLA2, this loop is composed of residues 99−118 (Figure 1). Since one edge of the loop comes quite close to the i-face near the active-site slot, a mutant bvPLA2 was made in which 99−118 was deleted, and the interfacial kinetics of this enzyme was studied. (2) The secreted PLA2 isozymes from Gila monster venom (*Heloderma suspectum*) have been purified and sequenced (*25*), and they show high homology to bvPLA2. Figure 1 shows the predicted structure of the i-face of one of the isozymes, Pa2, obtained by overlaying the homologous segments of the lizard enzyme onto the corresponding segments of bvPLA2. Like bvPLA2, Pa2 contains a ring of hydrophobic residues that surround the active-site slot, but unlike bvPLA2, the lizard enzyme contains only a single cationic residue (lysine-92) on its putative i-face. Thus it was of interest to study the kinetics of Pa2 on anionic vesicles, and the results of these studies are reported. (3) Manoalide and 12-*epi*-scalaradial (Chart 1) are aldehyde-containing marine natural products that have been shown to act as potent inactivators of secreted PLA2s by forming covalent adducts with one or more lysine residues (*26*−*30*). Manoalogue (Chart 1) is a synthetic analogue of manoalide, and it displays the same PLA2 inactivation properties as manoalide (*31*, *32*). In the present report, the abilities of manoalogue and 12-*epi*-scalaradial to inactivate the collection of lysine-to-glutamate bvPLA2 mutants were studied with the hope of better defining the mode of inactivation of bvPLA2 by these aldehydes.

Chart 1

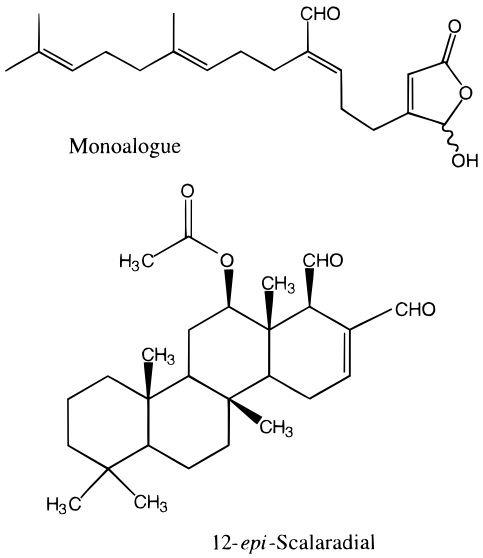

MATERIALS AND METHODS

Materials. All reagents and buffers used were analytical grade obtained from standard suppliers. The synthetic phospholipids dansyl-DHPE, DTPM, diC_6thioPC, and diC_6-thioPM were prepared as described (*24*, *33*). Other lipids were obtained from Avanti Polar Lipids. Manoalogue and 12-*epi*-scalaradial were obtained as gifts from Dr. Ed Mihelich (Lilly Labs, Indianopolis, IN) and Professor Robert Jacobs (University of California, Santa Barbara), respectively. Pa2 was obtained as a generous gift from Professor J. Christophe (Universite Libre de Bruxelles).

Purification of bvPLA2s. The bvPLA2 mutants were produced by a PCR-based method as described in Supporting Information (*1*−*3*). Proteins were produced in *Eeschericia coli* strain M15/pRep 4 and were purified, refolded, and

repurified as described (*2*). Most of the mutants were purified by ion-exchange chromatography on SP-Sephadex (*2*), but the mutants K85E/K94E/K133E, R23E/K85E/K133E, and E5 (K14E/R23E/K85E/K94E/K133E) do not bind to SP-Sephadex at high pH and were thus purified on an SP-Sephadex column (10 mL bed) equilibrated with 10 mM MES, pH 6.0. After loading and washing, the column was developed with a linear gradient of 10 mM MES, pH 6.0 (30 mL), to 10 mM MES, pH 6.0, and 1 M NaCl (30 mL). Active fractions were dialyzed against 1 mM Tris, pH 8.0, and concentrated in vacuo as described (*34*) or dialyzed against 10 mM Tris, pH 8.0, and concentrated using a Centriprep concentrator (Amicon). In general, vacuum concentration gave better recovery of bvPLA2. Concentrated protein solutions were stored at −20 °C and were stable indefinitely. The concentration of bvPLA2 was estimated either by UV spectroscopy [$E^{0.1\%}_{280nm} = 1.3$ (*32*)] or with the Bio-Rad protein assay kit (Bio-Rad, Richmond, CA) using, as a standard, a solution of commercial bvPLA2 (Boehringer Mannheim) that had been standardized by UV spectroscopy. All experiments described throughout this study with PLA2s were carried out at least twice to check for reproducibility, and many were carried out 3−4 times.

Kinetic Measurements. The hydrolysis of DMPM by bvPLA2 was measured using a pH-stat-based assay (*35*, *36*), and components of the mixture are given in the figure and table legends. Hydrolyses of diC_6thioPC and diC_6thioPM were monitored as described (*33*).

Inactivation Studies. As described (*32*), 10 mL of bvPLA2 (0.15 mg/mL in 10 mM Tris-HCl, pH 8.0) was mixed with 5 mL of manoalogue stock solution in DMSO (final manoalogue/bvPLA2 mole ratio was 20). Inactivation studies with 12-*epi*-scalaradial were carried out in the same way except that 2 mL of stock solution in DMSO was added to give a final 12-*epi*-scalaradial/bvPLA2 mole ratio of 10. Aliquots (3 mL) of reaction mixture were withdrawn 20, 50, and 120 min after addition of inactivator and added to a 4 mL pH-stat reaction mixture at 21 °C containing 0.6 mg DMPM as sonicated vesicles (small unilamellar vesicles), 20 of mg polymyxin B (Sigma), 2.5 mM $CaCl_2$, and 1 mM NaCl, pH 8.0. The initial velocity, recorded for several minutes was used to calculate the percent remaining enzymatic activity at each time point. The loss of enzymatic activity in control reactions over 120 min was less than 10%.

Binding of bvPLA2 to Phospholipid Vesicles. Vesicles of DTPM containing 3 mol % dansyl-DHPE were prepared by mixing stock solutions of lipids in chloroform in a glass tube. After complete removal of solvent in a Speed-Vac (Savant Inc.), water was added to give a suspension of 10 mg/mL lipid. Small unilamellar vesicles were prepared by sonication as described (*35*). Buffer (1−1.5 mL of 10 mM Tris-HCl, pH 8.0, 2 mM EDTA, and 2 mM EGTA or 10 mM Tris-HCl, pH 8.0, with various amounts of $CaCl_2$) with or without NaCl (from a 5 M stock) was placed in a quartz cuvette, and the desired additional components were added as specified in the figure captions. Fluorescence spectra were digitized during acquisition at a resolution of 0.5 nm, and spectra were corrected for baseline and dilution factors and normalized with spreadsheet software. The excitation and emission slit widths were 5 nm.

Analysis of Interfacial Binding by HPLC. HPLC was carried out using an alkyl-IAM column (IAM.PC.DD, 0.46 × 3 cm, Regis Technologies catalog no. 777007, s/n 100317) and an ester-IAM column (0.46 × 3 cm, Regis Technologies catalog no. 774010, s/n 100044). bvPLA2s (typically 2 μg in a 20 mL injected volume) were eluted with a linear gradient of 0−200 mM NaCl over 5−25 min in the mobile phase (45% acetonitrile in 1 mM EGTA and 10 mM Tris, pH 7.2) at a flow rate of 0.5 mL/min (at 25 min, elution with 200 mM NaCl was continued for an additional 25 min). Other solvents used are given in the Results section. Protein elution was monitored by UV absorbance and tryptophan fluorescence detectors in sequence.

RESULTS

Charge Reversal bvPLA2 Mutants Are Properly Folded. To test the role of cationic residues in promoting interfacial binding of bvPLA2, five of six basic residues on the putative i-face were individually mutated to glutamic acid (charge reversal). Single, double, triple, and quintuple-site mutants (Table 1) were characterized in detail. Mutation of R58 to glutamic acid resulted in a protein that did not refold in detectable amounts, and this problem was overcome by preparing R58A and multisite mutants containing R58A, which refolded with about a third of the yield obtained for wild type (WT). The six-site mutant E5/R58A did not refold. The role of the β-loop of bvPLA2 in supporting interfacial catalysis was examined with the D99−118 deletion mutant. This mutant refolded with about half the yield obtained for WT. The entire coding regions of all mutants (including those prepared by ligation of restriction fragments) were sequenced to verify that no additional mutations were present. All mutants gave a negative Ellman's test for free sulfhydryl groups, which indicates that all five disulfides present in native bvPLA2 were also present in the mutants. The circular dichroism spectra of all mutants were virtually superimposable on that of WT (not shown), as were the tryptophan fluorescence emission spectra (discussed later). These results show that at least the gross tertiary structures of the mutants are similar to that of WT.

Functional evidence that the mutants fold into a nativelike conformation comes from the kinetics of hydrolysis of short-chain phospholipids in the aqueous phase (i.e., with substrate concentrations well below their critical micelle concentrations). We have previously shown that bvPLA2 hydrolyzes diC_6-thioPC and diC_6-thioPM with apparent hyperbolic kinetics when the substrate concentrations are varied below their critical micelle concentrations (*33*), although we cannot rule out the possibility of enzyme−lipid microaggregation in such assays (*37*). Table 1 lists the turnover numbers for the hydrolysis of a fixed concentration (0.4 mM) of diC_6-thioPC or diC_6-thioPM by all bvPLA2 mutants. The turnover numbers for all mutants are 35−120% of the value for WT, and there were no discernible differences in the trends. These results establish that all mutants fold into a nativelike conformation that retain high specific activity on water-soluble substrates.

Inactivation of bvPLA2 by Reaction of Manoalogue and 12-epi-Scalaradial with K94. Previous studies have shown that treatment of secreted PLA2s with manoalogue and 12-*epi*-scalaradial leads to covalent modification of one or more lysines. As a direct test of the idea that inactivation is due to lysine modification and that surface lysine residues are

Table 1: Initial Velocities for the Hydrolysis of Water-Soluble and Vesicular Substrates by WT and Mutant bvPLA2s

	substrate								
bvPLA2	diC$_6$thioPM initial velocity (% of WT)	diC$_6$thioPC initial velocity (% of WT)	DMPM initial velocity (% of WT)	N_S on DMPM (% of WT)	k_i on DMPM (% of WT)	K_{Ca}, K_{Ca}*(DTPM) (μM)	$X_I(50)$ for HK-42 mole fraction[a]	k_d[b] (min^{-1})	peak elution times[c] ester-IAM column (min)
WT	100 (14 s^{-1})[d]	100 (6 s^{-1})	100 (80 s^{-1})	100 (10 000)	100 (0.001 s^{-1})	190 ± 10, 5.6 ± 0.6	0.00025 (0.00027)	0.005 [<0.001]	16.2 (1.22)
K14E	52	69	80	88	95				12.25 (0.417)
R23E	54	40	95	82	95				13.45 (0.55)
R58A	48	50	80	96	90				
K85E	50	90	77	95	88				12.67 (0.167)
K94E	44	55	58	79	82				
K133E	42	54	54	82	85				14.43 (0.517)
K14E/R23E	58	52	103	82	85				16.62 (1.10)
R23E/R58A	65	67	87	80	82				
K85E/K133E	86	85	103	95	88				14.85 (0.285)
K14E/R23E/R58A	80	120	40	90	80				
R23E/K85E/K133E	91	83	80	84	94	250 ± 25, 24 ± 4	0.00052 (0.00080)	0.042	11.98 (0.15)
K85E/K94E/K133E	50	58	75	81	84		0.00047	[0.006]	10.45 (0.15)
E5	95	35	95	90	85	160 ± 20, –	0.00040	0.021 [0.014]	10.85 (0.267)
Δ99−118 Pa2	56	78 (1.3 s^{-1})	70 (13 s^{-1})	90	88				

[a] Numbers in parentheses are the $X_I(50)$ values in the presence of 0.4 M NaCl. All $X_I(50)$ values have an error of ±20% or less. [b] Numbers not in brackets are derived from Figure 5, and numbers in brackets are derived from Figure 6. [c] Peak retention times with NaCl gradient elution (0−200 mM) or isocratic NaCl elution (200 mM, numbers in parentheses). [d] Numbers in parentheses are the actual turnover numbers for WT bvPLA2 and Pa2.

important for interfacial catalysis by bvPLA2, inactivation studies were carried out with the panel of lysine-to-glutamate mutants. With manoalogue and 12-*epi*-scalaradial (inactivation curves given as Supporting Information), K94E was completely resistant to inactivation, K85E was slightly resistant to inactivation, and all other mutants became inactivated with the same kinetics as WT.

Charge Reversal and Δ99−118 bvPLA2 Mutants Are Fully Functional on Anionic Vesicles. Secreted PLA2s including bvPLA2 hydrolyze all of the phospholipids in the outer monolayer of anionic vesicles without leaving the vesicle surface (scooting mode) because the residence time of the enzyme on anionic vesicles of phospholipids such as DMPM is longer than the time needed to hydrolyze all of the outer layer substrates (*22*, *23*, *36*). In the scooting mode with more vesicles than enzymes, the reaction ceases before all vesicles are hydrolyzed because enzyme does not hop between vesicles. With small unilamellar vesicles, the reaction progress curve has a first-order appearance because the surface concentration of substrate that the bound enzyme "sees" (expressed as mole fraction of substrate in the interface) is decreasing rapidly (Figure 2 and ref *36*). Remarkably, all of the mutants prepared in this study yield reaction progress curves that are very similar to that obtained with WT (shown in Figure 2 for WT, R23E/K85E/K133E, K85E/K94E/K133E, and E5; other mutants not shown). These first-order curves are characterized by the quantities N_S and k_i, where N_S is the amount of product formed at the end of the reaction and k_i is the exponential constant ($e^{-k_i t}$) (*10*). N_S and k_i values are listed in Table 1. *These results establish that cationic lysine and arginine residues on the putative i-face of bvPLA2 are not required for scooting-mode hydrolysis of DMPM vesicles.* Δ99−118 also operates on DMPM vesicles in the scooting mode, and thus it is clear

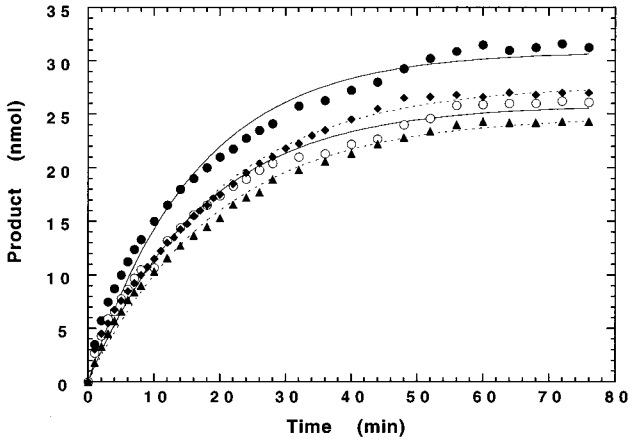

FIGURE 2: DMPM reaction progress curves: WT (●, solid line); R23E/K85E/K133E (○, solid line); K85E/K94E/K133E (▲, dashed line); and E5 (◆, dashed line). The lines are the regression fit of the data to the first-order equation $P_t = P_{max}(1 - e^{-kt})$. pH-Stat reaction mixtures contained 4 mL of 250 μM DMPM small unilamellar vesicles, 0.6 mM $CaCl_2$, 1 mM NaCl, and 50 ng of enzyme at pH 8.0, 21 °C.

that the β-loop is not essential for high-affinity binding to anionic vesicles. The fact that N_S is similar for WT and all mutants shows that all proteins are completely folded into a nativelike conformation and that the enzymatic activity being measured is not due to low-level contamination from another PLA2.

Another reason for the cessation of reaction progress prior to total substrate consumption is that the enzyme may become inactivated during the reaction. For WT, this has been ruled out on the basis of the observation that addition of high Ca^{2+} (2.5 mM) after the initial reaction on DMPM vesicles ceases leads to immediate initiation of the reaction progress (*36*). High Ca^{2+} causes fusion of DMPM vesicles

(*38*, *39*) and allows the bound enzyme to come in contact with excess substrate. Similar findings were obtained in the present study with the mutants (not shown). Furthermore, with the multisite mutants, addition of NaCl leads to reinitiation of the reaction after it ceases in the absence of salt (discussed below), presumably due to salt-induced hopping of enzyme between vesicles (*24*).

The reaction kinetics were also studied under zero-order conditions to obtain the initial velocity for the hydrolysis of DMPM vesicles in the scooting mode. This is carried out by including the cationic peptide polymyxin B in the reaction mixture. This agent causes rapid intervesicle exchange of DMPM and its PLA2 reaction products, and this keeps the mole fraction of substrate close to its initial value of unity (*39*−*41*). The data in Table 1 shows that the initial velocities per enzyme for the hydrolysis of DMPM are very similar for WT and all mutants. This result also shows that the enzymes do not inactivate on DMPM vesicles.

The ability of the competitive inhibitor HK-42 (*3*) to block scooting-mode hydrolysis of DMPM catalyzed by the mutants was quantified with the PxB/DMPM assay. The mole fractions of HK-42 required for a 2-fold decrease in the initial reaction velocity, $X_I(50)$, are virtually the same for WT, R23/K85/K133, K85E/K94E/K133E, and E5 (Table 1). Collectively, these results show that inhibitor binding to bvPLA2 at the anionic interface is not influenced by the charge-reversal mutations.

The surprisingly high activity of E5 on anionic vesicles was confirmed with three independent preparations of this mutant, each made from a different *E. coli* clone. The bvPLA2 gene from each of the three clones was sequenced to verify that all five mutations were present. E5 elutes from a C4 reverse-phase HPLC column 3 min later than WT under the conditions described previously (*32*), no OD_{280} peak was detected in the region where WT elutes, and all of the enzymatic activity elutes with the late peak (not shown). Finally, the elution properties of the triple-site mutants and E5 versus WT from ion-exchange columns is consistent with the higher anionic surface charge of the mutants.

Multisite, Charge Reversal bvPLA2 Mutants Display Normal Ca^{2+} Binding and Ca^{2+}-Promoted DTPM Binding in the Active Site. The affinities of WT, R23E/K85E/K133E, and E5 in aqueous solution for Ca^{2+} were determined by spectral titration; Ca^{2+} binding causes a small reduction in tryptophan emission (*36*). Experiments were carried out with 4 μM enzyme in 10 mM Tris-HCl, pH 8.0, with excitation at 280 nm and emission at 335 nm. The data fit well to the standard binding equation (hyperbolic response), and values of the dissociation constant for the E·Ca^{2+} are 0.19 mM for WT [this agrees well with the previous value of 0.32 mM (*36*)], 0.25 mM for R23E/K85E/K133E, and 0.16 mM for E5. Thus, the multisite mutations have virtually no effect on binding of Ca^{2+} to enzyme in the aqueous phase, again showing that the proteins are properly folded.

Ca^{2+} is required for the binding of active-site-directed ligands to bvPLA2 bound to vesicles but not for the binding of enzyme in the aqueous phase to vesicles (*14*, *36*). The relevant equilibria are

$$E{\cdot}Ca^{2+} \overset{n\mathrm{L}}{\rightleftharpoons} E^*{\cdot}Ca^{2+} \overset{\mathrm{DMPM}}{\rightleftharpoons} E{\cdot}Ca^{2+}{\cdot}\mathrm{DMPM}$$

Here, E·Ca^{2+} is the enzyme-Ca^{2+} complex in the aqueous phase, E*·Ca^{2+} is the corresponding complex at the interface, E*·Ca^{2+} ·DMPM is the Michaelis complex at the interface, and *n*L is the enzyme binding site on the vesicle composed of *n* lipids. In the presence of vesicles of DTPM, a nonhydrolyzable analogue of DMPM, the affinity of the enzyme for Ca^{2+} is dictated by the equilibrium K_{Ca}*(DTPM) for the dissociation reaction E*·DTPM·Ca^{2+} ⇄ E* + Ca^{2+} (*36*).

Table 2: Fluorescence Spectral Properites of WT and Mutant bvPLA2s

	λ_{max} (nm), relative intensity		
	trytophan emission[a] (ex 292 nm)	dansyl emission[b] (ex 340 nm)	energy transfer[c] (ex 292 nm)
vesicles only		528, 1.0	
vesicles only + NaCl		528, 0.95	
	WT		
E	338, 1.0		
E·Ca^{2+} [d]	338, 0.85		
E*	337, 1.0	508, 1.45	493, 1.0
E* + NaCl[d]	337, 1.0	512, 1.40	499, 0.80
E*·Ca^{2+}	338, 0.88	nd	nd
E*·Ca^{2+} + NaCl	nd[e]	nd	nd
	R23E/K85E/K133E		
E	339, 0.95		
E·Ca^{2+}	339, 0.80		
E*	339, 0.95	512, 1.28	504, 0.83
E* + NaCl	339, 0.95	523, 1.10	519, 0.32
E*·Ca^{2+}	339, 1.47	511, 1.25	505, 0.80
E*·Ca^{2+} + NaCl	nd	524, 1.12	519, 0.30
	E5		
E	339, 0.92		
E + Ca^{2+}	339, 0.76		
E*	338, 0.92	510, 1.45	495, 0.84
E* + NaCl	338, 0.92	520, 1.20	506, 0.45
E*·Ca^{2+}	338, 0.96	nd	nd
E*·Ca^{2+} + NaCl	nd	nd	nd

[a] Relative intensities for all proteins are reported relative to that of the E form of WT (unity intensity). [b] Measured with vesicles saturated with enzyme. Relative intensities are reported relative to the intensity of vesicles in the absence of enzyme (unity intensity). [c] Intensities are the energy transfer signal measured under the stated conditions minus the signal from vesicles alone under the same conditions. Relative intensities (given in the table) are reported relative to the E* form of WT in the absence of NaCl and Ca^{2+} (unity intensity). [d] Ca^{2+} and NaCl are present at saturating levels. [e] nd, not determined.

The facts that HK-42 inhibits WT and R23E/K85E/K133E equally well (Table 1) and that binding of this compound to the active site of E* requires Ca^{2+} strongly suggests that Ca^{2+} binding to the mutant is not perturbed. Ca^{2+} binding to the E* form on DTPM was also studied by monitoring tryptophan emission as a function of bulk Ca^{2+} concentration (Table 2; spectral titrations given as Supporting Information). With WT, a small decrease in tryptophan emission occurs (like with the E form), and constant K_{Ca}*(DTPM) = 5.6 μM is obtained from the fit of the data to a hyperbola. Note that K_{Ca}*(DTPM) is much less than K_{Ca} = 190 μM measured for the E form (see above), and this is because of the synergism between Ca^{2+} and DTPM active-site binding (*14*, *36*). Interestingly, addition of Ca^{2+} to R23E/K85E/K133E bound to DTPM vesicles led to a hyperbolic increase in tryptophan emission, and K_{Ca}*(DTPM) = 24 μM was obtained. The fact that synergism between Ca^{2+} and DTPM active site binding is seen with this triple mutant (K_{Ca} = 250 μM), although somewhat less so than with WT, strongly suggests that substrate binding is not significantly compromised in the multisite mutant. Virtually no change in

tryptophan emission was seen when Ca^{2+} was added to E5 bound to DTPM vesicles. The reason for the differences in intensity changes with added Ca^{2+} among the three proteins is not known. In general, the effect of Ca^{2+} binding on the emission intensity of a tryptophan distant from this metal (as is the case with bvPLA2) is difficult to predict and is probably due to subtle changes in the electrostatic potential surrounding tryptophan.

Since the reaction velocities for the action of WT and charge reversal mutants on DMPM vesicles are all similar and since substrate and Ca^{2+} are not noticeably perturbed, it may be concluded that the interfacial turnover numbers, k_{cat}*, for all of these proteins are similar.

Charge Reversal bvPLA2 Mutants Bind with High Affinity to Anionic Vesicles. Binding studies by fluorescence resonance energy transfer using 3 mol % dansyl-DHPE in DTPM are summarized in Figure 3. Calcium was omitted (2 mM EDTA and 2 mM EGTA) so that DTPM binding in the active site was prevented, and thus only the E to E* step was being studied. These studies were carried out by adding increasing amounts of bvPLA2 to a fixed amount of lipid present as vesicles. Remarkably, all of the mutants prepared in this study readily bind to anionic DTPM vesicles. Figure 3A shows that the binding curves with 100 μM total lipid for all single-site mutants are virtually identical to that for WT. Binding of multisite mutants R23E/K85E/K133E, K85E/K94E/K133E, and E5 as well as WT is shown in Figure 3B. These studies were carried out with 25 μM total lipid and remarkably, even under these conditions, the multisite mutants, like WT, bind tightly to anionic DTPM vesicles. The binding data were fit by nonlinear regression to the mass action equation for binding of bvPLA2 to independent sites on a vesicle composed of n phopsholipids (*42*), and it was found that values of the E* to E dissociation constant, K_d, are <1 μM for WT and all mutants. Thus the binding is too tight to accurately determine K_d since $[L_T] \gg 1$ μM. Values of n are in the range 15−20, and thus 1 bvPLA2 shields about 15−20 outer vesicle layer lipids. This number is similar to 30 lipids/enzyme for the binding of porcine pancreatic PLA2 to DTPM vesicles (*10*). In principle, one could use lower lipid concentrations to better determine K_d values, but the fluorescence energy transfer method is not sensitive enough for this. For example, with 2 μM total lipid (<0.2 nM vesicles), one must use no more than 50 nM bvPLA2 (each enzyme shields about 20 phospholipids), and roughly half of the lipid is in the outer vesicle monolayer. Furthermore, no more than 5−10 nM enzyme should be used if crowding effects are to be avoided. Fluorescence energy transfer under such dilute conditions is difficult to detect.

Energy transfer measured when the triple mutants R23E/K85E/K133E and K85E/K94E/K133E bind to DTPM/dansyl-DHPE vesicles show that values of F/F_0 reached when vesicles are saturated with enzyme are considerably smaller than F/F_0 for WT and E5, although all of the mutants give the same F/F_0 response in the range of 0−10 μg of protein added (Figure 3B). This shows that under conditions of noncrowding of enzyme on vesicles, the energy transfer efficiency is the same for all proteins, suggesting that they sit on the vesicles in a similar fashion. Possible reasons for the lower efficiency of energy transfer for the triple mutants under crowded conditions are given in the Discussion section.

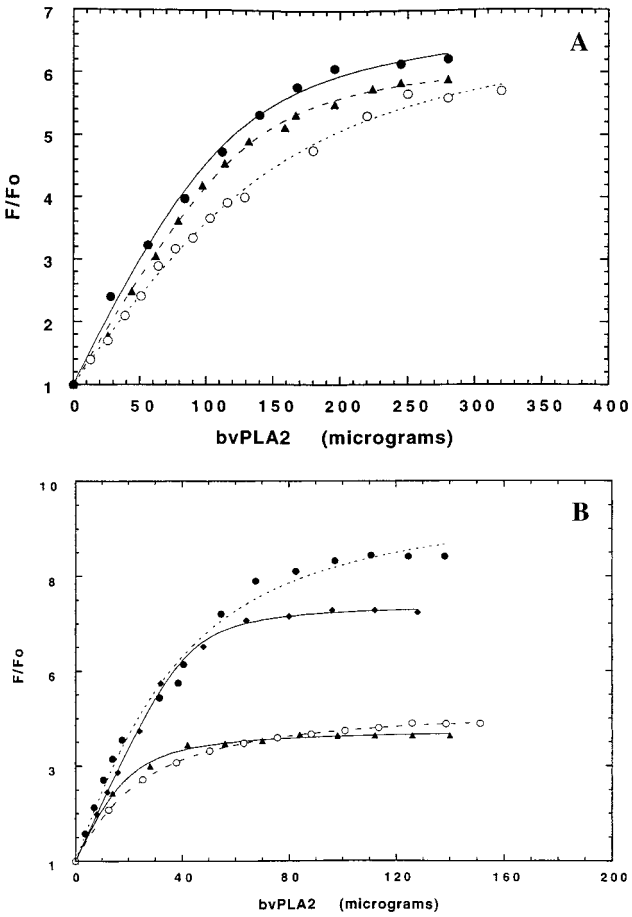

FIGURE 3: Binding of bvPLA2s to DTPM vesicles. Binding experiments were carried out at 25 °C with sonicated vesicles of DTPM containing 3 mol % dansyl-DHPE in 1.5 mL of 10 mM Tris-HCl, pH 8.0, 2 mM EDTA, and 2 mM EGTA. The indicated amount of bvPLA2 was added, and the fluorescence at 500 nm was monitored with excitation at 280 nm (resonance energy transfer). Data are plotted as the emission at 500 nm (F) divided by the emission at 500 nm in the presence of vesicles but not enzyme (F_0). (A) ●, WT; ▲, R23E; ○, K133E, all with 100 μM total lipid. (B) ●, WT; ▲, R23E/K85E/K133E; ○, K85E/K94E/K133E; ◆, E5, all with 25 μM total lipid.

As reported previously, binding of bvPLA2 to zwitterionic DTPC/dansyl-DHPE vesicles is too weak to be detected by energy transfer even with 100 μM lipid. Similarly, all of the multisite mutants failed to bind to DTPC/dansyl-DHPE when present at 100 μM total lipid in the cuvette (not shown).

bvPLA2s Remain Bound to Anionic Vesicles in the Presence of NaCl. The effect of NaCl on bvPLA2s bound to DTPM vesicles was monitored to explore the electrostatic component of interfacial binding (*24*). bvPLA2s were prebound to DTPM/dansyl-DHPE vesicles under noncrowding conditions, and fluorescence resonance energy transfer was monitored as a function of salt concentration. With WT, all single-site mutants, and K14E/R23E, up to 500 mM NaCl caused <10% change in F/F_0 (Figure 4A), showing that these proteins do not significantly desorb from DTPM vesicles. In contrast, the multisite mutants R23E/K85E/K133E, K85E/K94E/K133E, and E5 display a significant salt-dependent decrease in energy transfer intensity (Figure 4B). Note that the two triple-site mutants show a more pronounced salt effect than does E5. In all cases, the effect of NaCl reaches a limiting plateau well above the value of the fluorescence in the absence of enzyme. An independent control showed

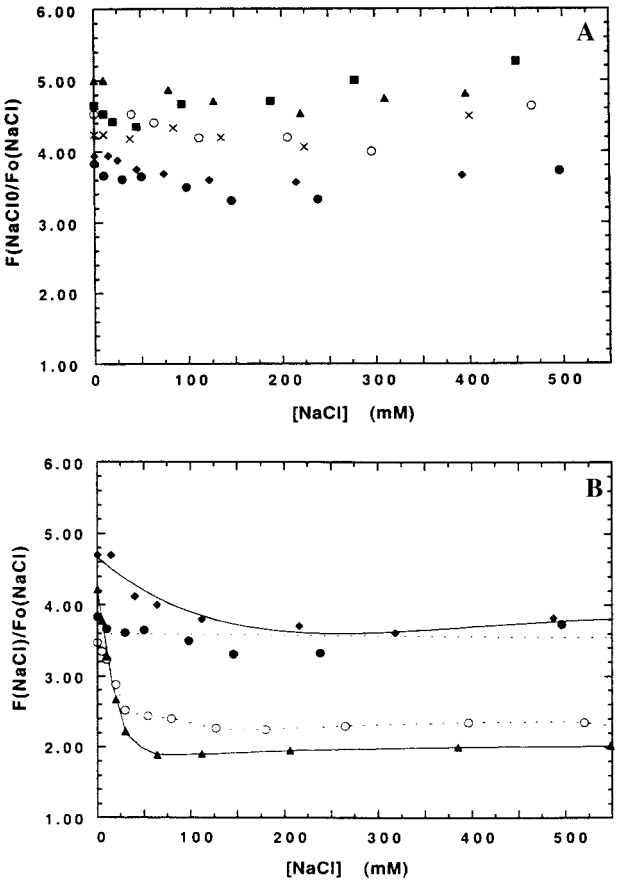

FIGURE 4: Effect of NaCl on binding of bvPLA2 to DTPM vesicles. bvPLA2s (10 μg) were prebound to DTPM vesicles (25 μM) under conditions as in Figure 3B. The indicated amount of NaCl was added, and the fluorescence at 500 nm was followed with excitation at 280 nm (resonance energy transfer). F(NaCl) is the fluorescence intensity in the presence of enzyme, vesicles, and various amounts of NaCl, and F_0(NaCl) is the corresponding intensity in the absence of enzyme. F_0(NaCl) decreased by less than 30% as NaCl was increased from 0 to 500 mM. (A) ●, WT; ○, K14E; ▲, R23E; ◆, K85E; ×, K133E; ■, K14E/R23E. (B) (●, dotted line, WT; ▲, solid line, R23E/K85E/K133E; (○, dotted line), K85E/K94E/K133E; ◆, solid line, E5.

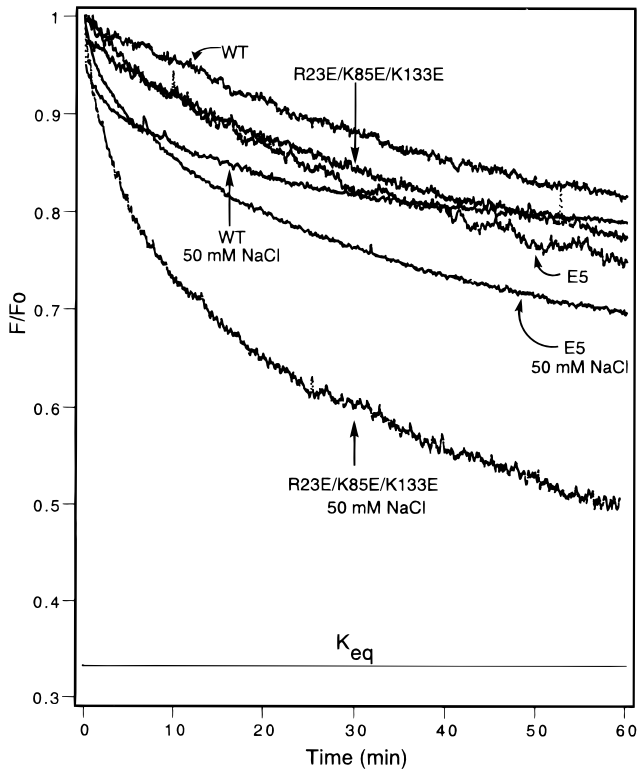

FIGURE 5: Intervesicle exchange of bvPLA2s between DTPM vesicles. Mixtures contained 1 mL of 10 mM Tris, pH 8.0, 86 μM DTPM/dansyl-DHPE vesicles, and 0 or 50 mM NaCl and were stirred at 25 °C. Enzyme (0.28 μM) was added last. Fluorescence energy transfer was monitored as in previous experiments, and after a stable baseline was reached, 172 μM DTPM vesicles were added and the energy transfer was monitored for 1 h. The K_{eq} lines are the values of F/F_0 expected if all of the enzyme redistributes on vesicles.

that added NaCl has little effect on the fluorescence of DTMP/dansyl-DHPE vesicles alone.

The 30−70% decrease in energy transfer (Figure 4B) could be due to an increase in the donor−acceptor distance, an increase in the polarity of the intervening dielectric, or a change in relative orientation of the donor and acceptor. The possibility that tryptophan emission is perturbed in the mutants was investigated by obtaining the tryptophan emission spectra for WT, R23E/K85E/K133E, and E5 in solution and bound to DTPM/dansyl-DHPE vesicles with and without NaCl. The tryptophan emission spectra of the three proteins in aqueous solution are virtually identical (Table 2; spectra given as Supporting Information). Although the figure shows the normalized spectra, the specific molar emission intensities were essentially identical (<10% variation) for all three proteins. The tryptophan emission spectra are not noticeably perturbed when 0.4 M NaCl is added (spectra given as Supporting Information). The tryptophan emission spectra of WT, R23E/K85E/K133E, and E5 in solution, bound to DTPM vesicles, and bound to vesicles in the presence of 0.4 M NaCl are virtually identical (Table 2; spectra given as Supporting Information). Together, these studies provide additional confirmation that the multisite mutants are properly folded, and they show that the change in energy transfer upon addition of NaCl (Figure 3) is not due to alteration in tryptophan emission.

The $X_I(50)$ values for the inhibitor HK-42 interacting with WT and the multisite charge reversal mutants do not change in the presence of NaCl (Table 1). This result shows that phospholipid and Ca^{2+} binding in the active site of the E* form is not affected by NaCl.

Multisite Charge Reversal bvPLA2 Mutants Dissociate Slightly Faster than WT from Anionic Vesicles. Although only an upper limit of $K_d = 1$ μM could be obtained from the energy transfer binding experiments, it was possible to measure the rate of exchange of enzyme between DTPM vesicles. The decrease in energy transfer from DTPM/dansyl-DHPE vesicles containing bound enzyme under noncrowding conditions was monitored after the addition of an excess of nonfluorescent DTPM and in the absence of Ca^{2+} (Figure 5). The multisite mutants dissociate slightly faster than does WT, showing that their interfacial binding is modestly perturbed.

As also shown in Figure 5, the presence of 50 mM NaCl increases the rate of intervesicle exchange for all proteins but more so for the multisite mutants than for WT (R23E/K85E/K133E faster than E5 faster than WT). Values of the vesicle desorption rate constants, k_d, were estimated from the initial slopes and are listed in Table 1. Thus, with the multisite charge reversal mutants, NaCl has the double effect

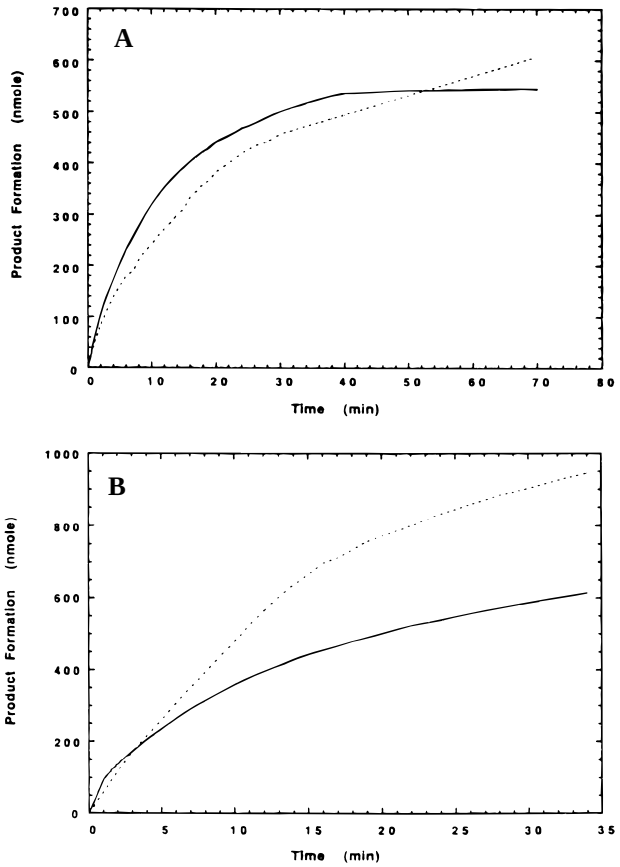

FIGURE 6: NaCl-induced intervesicle exchange of bvPLA2s on DMPM vesicles (kinetic method). (A) Progress curves for E5 (0.15 μg), in the absence (solid line) and presence (dashed line) of 200 mM NaCl, acting on 250 μM DMPM in 4 mL of 1 mM NaCl and 0.6 mM $CaCl_2$, pH 8.0, 21 °C in the pH-stat reaction vessel. (B) Same as for panel A but with K85E/K94E/K133E.

of decreasing the efficiency of energy transfer between tryptophan and dansyl-DHPE present in the vesicles (Figure 3) and of increasing the rate of vesicle desorption, and these effects are much less pronounced with WT.

Intervesicle exchange was also studied under lipolytic conditions with DMPM vesicles. Addition of up to 300 mM NaCl did not cause reinitiation of the reaction of WT acting on DMPM vesicles in the scooting mode after the initial reaction had ceased as in Figure 2 (not shown). This is consistent with the lack of effect of NaCl on energy transfer (Figure 4) and on the desorption from DTPM vesicles (Figure 5). In contrast, as shown in Figure 6 for K85E/K94E/K133E and E5, the presence of 200 mM NaCl in DMPM reaction mixtures prior to the addition of enzyme causes transfer of bound enzyme to excess vesicles. Estimates of the rate constant for interfacial desorption, k_d, come from fitting the progress curves to eq 10 of ref *39*, and values are listed in Table 1. The value of k_d for E5 in the presence of 200 mM NaCl and 0.6 mM $CaCl_2$ of 0.014 min^{-1} is not very different from the value of k_d of 0.021 min^{-1} measured with DTPM vesicles in the presence of 50 mM NaCl and in the absence of $CaCl_2$ (Figure 5).

Multisite Charge Reversal bvPLA2 Mutants Bind More Weakly to an Immobilized Membranelike Surface, and Binding Requires Glycerol Esters. An independent assessment of the binding of bvPLA2s to the interface was obtained from HPLC experiments. Two types of zwitterionic columns

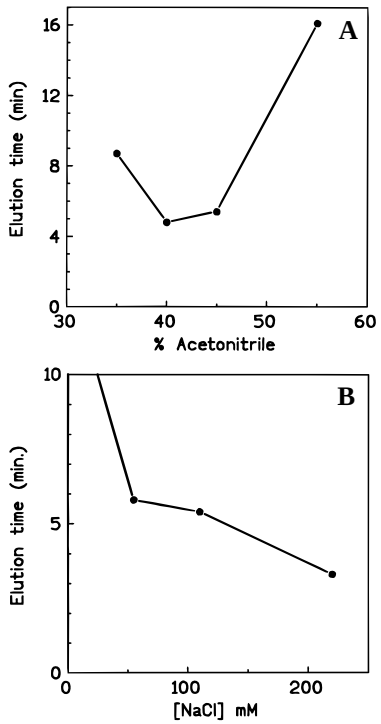

FIGURE 7: Peak retention times of bvPLA2s from the ester-IAM HPLC column. The mobile phase is 10 mM Tris, pH 7.2, 1 mM EGTA, 110 mM NaCl, and the indicated amount of CH_3CN (A) or 10 mM Tris, pH 7.2, 1 mM EGTA, 45% CH_3CN, and the indicated amount of NaCl (B). The retention time in the absence of NaCl and in the presence of 45% CH_3CN is 60 min.

were used. The alkyl-IAM column contains a close-packed layer of the single-chain amphiphile decylphosphorylcholine. The amphiphile contains an ω-carboxyl group amide linked to propylamine on the solid support. The ester-IAM column contains dipalmitoyl phosphatidylcholine linked in the same way via an ω-carboxyl group on its *sn*-2 chain. Both HPLC columns were judged to contain about 2% surface anionic charge. This was estimated from the shape of the elution profile for tris(2,2′-bipyridine)ruthenium chloride (Aldrich) (*43*). These experiments were carried out in the absence of Ca^{2+} (1 mM EGTA in the mobile phase) so that only the E to E* equilibrium is being monitored. Furthermore, porcine pancreatic and snake venom PLA2 do not hydrolyze the *sn*-2 ester of the ester-IAM column (*44*), and we have confirmed this with bvPLA2 (not shown). This is presumably because a phosphatidylcholine cannot leave the plane of the monolayer to bind to the active site of the enzyme.

In aqueous buffer without NaCl or CH_3CN, WT bvPLA2 did not bind to the alkyl-IAM column, and in marked contrast, no elution over 30 min was seen with the ester-IAM column. The retention of WT on the ester-IAM column was further investigated using mobile phases of increasing organic solvent and NaCl. As shown in Figure 7A, in the presence of 100 mM NaCl, the elution time of WT from the ester-IAM column depends in a biphasic fashion on the percent CH_3CN in the mobile phase. As shown in Figure 7B, in the presence of 45% CH_3CN, elution is faster as the salt concentration is increased. As discussed later, these results suggest that ionic and hydrogen-bonding effects are responsible for binding of bvPLA2 to the ester-IAM column.

To evaluate the interfacial binding of the multisite charge reversal mutants, we determined their retention times from

the ester-IAM column in the presence of buffer containing 45% CH_3CN and with isocratic elution with 200 mM NaCl or with a 0−200 mM NaCl gradient (Table 1). These conditions are sufficient to elute WT (Figure 7), and the retention times measured with a NaCl gradient should distinguish the effect of mutation on electrostatic interfacial binding. Electrostatic binding to the ester-IAM column is possible because of the presence of a small amount of interfacial anions on the solid support as noted above. If charge reversal mutation reduces the electrostatic interfacial binding component, the HPLC elution time should be shortened. The retention times for all proteins with isocratic or gradient NaCl elution show the same trend, suggesting that NaCl competes for the ionic interactions between the enzyme and the interface. The retention times of the mutants are, in general, shorter than that of WT, and the multisite mutants R23E/K85E/K133E, K85E/K94E/K133E, and E5 have the shortest retention times (Table 1). Of the single-site mutants, K14E has the shortest retention time, and it is curious that the double mutants K14E/R23E and K85E/K133E elute later than the single-site mutants. Qualitatively, these results show that the lysine and arginines on the putative i-face of bvPLA2 do make some contribution to the overall interfacial binding and that the contribution of certain residues is more significant than of others. These results qualitatively confirm the fluorescence energy transfer results; however, it is difficult to make a quantitative comparison because the energetics of interface binding cannot readily be extracted from results of either of these two methods.

Anomalous Behavior of bvPLA2 Charge Reversal Mutants When Crowded on Anionic Vesicles. Crowding effects of the multisite charge reversal mutants were noted as a lower efficiency of energy transfer in vesicle binding studies (Figure 3B). This was explored further by obtaining the dansyl emission spectra (excitation at 340 nm) of DTPM/dansyl-DHPE vesicles alone and saturated with WT, R23E/K85E/K133E, and E5 (crowded conditions, Figure 8 and Table 2). Dansyl emission from vesicles in the absence of enzyme is hardly perturbed by the addition of 0.4 M NaCl. In the absence of salt, addition of WT causes the dansyl emission intensity to increase 45%, and the λ_{max} shifts from 528 to 508 nm. This shift is consistent with the environment of the dansyl probe becoming more shielded from water as it contacts enzyme at the interface (*17*). Addition of 0.4 M NaCl causes a slight shift in λ_{max} from 508 to 512 nm, and the intensity falls only slightly. Thus, NaCl does not cause a significant change in the microinterface between vesicle and WT, consistent with the lack of salt effect on energy transfer (Figure 4B). As shown in Figure 8B, R23E/K85E/K133E behaves very differently. Upon binding, λ_{max} shifts from 528 to 512 nm (smaller shift than with WT) and the emission intensity increases 28%. Addition of 0.4 M NaCl causes a significant reduction in the intensity and λ_{max} shifts to 523 nm. These results argue that the extent of dansyl desolvation when R23E/K85E/K133E binds in the absence of salt is less than that which occurs when WT binds, and they are consistent with the diminished energy transfer maximum for the triple-site mutant compared to WT (Figure 3B). The dramatic effect of NaCl on dansyl emission is also consistent with the effect of salt on energy transfer (Figure 4B). Finally, the fact that the dansyl emission spectrum of vesicles coated with R23E/K85E/K133E in the presence of 0.4 M NaCl (sufficient to give a maximal spectral change, Figure 4B) is distinct from the spectrum of vesicles plus salt alone proves that the enzyme has not left the interface. E5 shows behavior intermediate between that of WT and the triple-site mutant (Figure 8C). Dansyl emission spectra via energy transfer (excitation at 292 nm; spectra given as Supporting Information) are consistent with what was

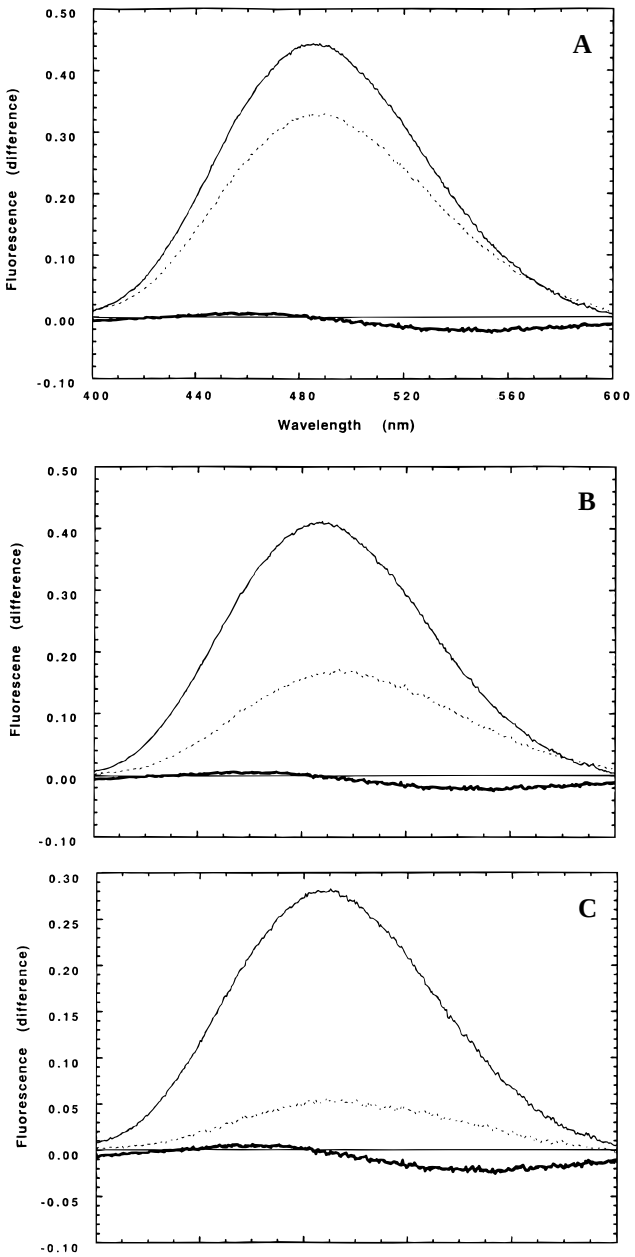

FIGURE 8: Dansyl emission difference spectra (excitation at 340 nm, emission at 400−600 nm) in 10 mM Tris-HCl, 2 mM EDTA, and 2 mM EGTA, pH 8.0 at 25 °C. In all spectra, the bold solid line is the emission spectrum of 25 μM DTPM/dansyl-DHPE vesicles in the absence of enzyme and in the presence of 0.4 M NaCl minus the spectrum of vesicles alone in the absence of NaCl. The horizontal solid line marks the zero difference line. (A) Emission spectrum of 100 μg of WT bound to 25 μM DTPM/dansyl-DHPE vesicles minus the spectrum of vesicles alone (solid line). The dotted line is the emission spectrum of WT bound to vesicles in the presence of 0.4 M NaCl minus the spectrum of vesicles alone in the absence of NaCl. (B) Same as in panel A except with R23E/K85E/K133E. (C) Same as in panel A except with E5. Spectra are not normalized.

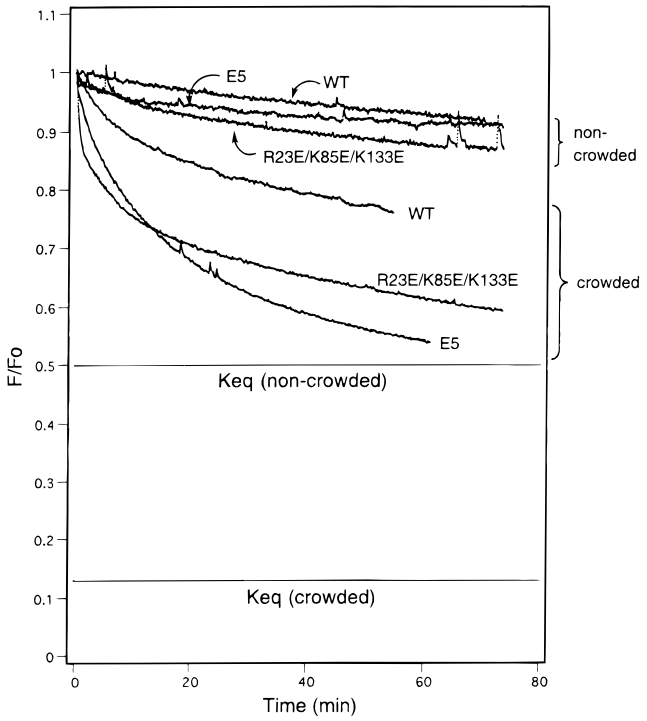

FIGURE 9: Intervesicle exchange from DTPM vesicles under crowded conditions. The indicated bvPLA2s were prebound to DTPM/3% dansyl-DHPE vesicles under crowded conditions (26 μM total lipid, 0.6 μM enzyme) in 10 mM Tris, pH 7.6. Energy transfer (excitation at 280 nm, emission at 500 nm) was followed at 25 °C after the addition of 175 μM DTPM vesicles without dansyl-DHPE. The horizontal lines (K_{eq}) show the energy transfer expected if all of the enzyme redistributes on vesicles.

observed for dansyl emission from direct excitation (Figure 8; see also Table 2).

As shown in Figure 9, intervesicle exchange between DTPM vesicles appears faster for all proteins under crowded conditions, and both R23E/K85E/K133E and E5 appear to desorb from vesicles faster than WT. Under crowded conditions, the decrease in energy transfer is multiexponential; there is a fast phase at early times that gives way to a slower phase, and the fast phase is most pronounced with R23E/K85E/K133E and least pronounced with WT. Under noncrowding conditions (Figure 5), the fast phase is barely detected.

Studies with Pa2. Because the Gila monster PLA2 contains only the single basic residue K92 on its putative i-face (Figure 1), it was of interest to study the kinetic properties of Pa2 acting on anionic vesicles. As shown in Figure 10, Pa2 shows anomalous kinetic behavior when added to a reaction mixture containing DMPM, polymyxin B, and Ca^{2+}. An initial burst of activity is seen in the first few minutes and this gives rise to a slow phase that accelerates over time. Product activation was ruled out by the fact that the same lag was seen when DMPM vesicles containing 10 mol % products (1:1 mixture of myristic acid and 1-myristoyl-*sn*-lysophosphatidylmethanol) were used (not shown). Evidence of slow binding of Pa2 to DMPM vesicles comes from the following experiment. When Pa2 was preincubated with 0.1 mg of DMPM vesicles in the presence of Ca^{2+} for 30 min, the reaction began immediately after addition the remaining portion of DMPM (0.5 mg), additional Ca^{2+} (2.5 mM final concentration), and polymyxin B (Figure 10). Polymyxin B is added to promote rapid

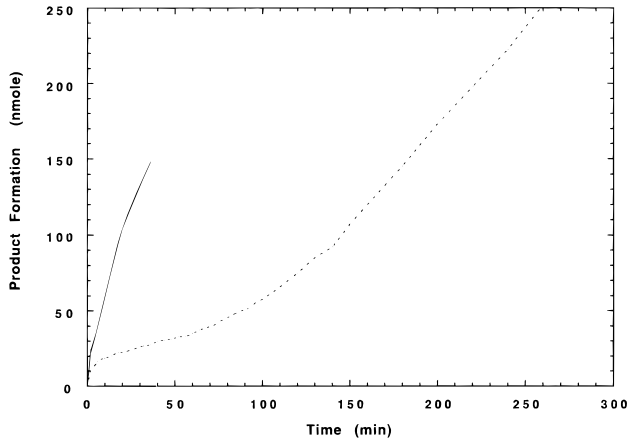

FIGURE 10: DMPM reaction progress curves with Pa2. (A) pH-Stat reaction mixtures contained 4 mL of DMPM small unilamellar vesicles (250 μM), 1 mM NaCl, 2.5 mM $CaCl_2$, and 20 mg/mL PxB at pH 8.0 and 21 °C and 1.8 μg of Pa2 (dotted line) or 1.8 μg of Pa2 preincubated with a 20% portion of DMPM before measuring the reaction after adding PxB and the remaining portion of DMPM (see Results) (solid line).

intervesicle exchange of DMPM, which ensures that Pa2 sees the full portion of substrate (0.6 mg); however, omission of polymyxin B did not have a noticeable effect, which suggests that Pa2 is not irreversible bound to DMPM vesicles. The latter result is also supported by the observation that all vesicles become hydrolyzed even when the number of vesicles exceeds the number of Pa2 molecules (hopping mode catalysis, not shown). Pa2 may exist in an aggregate form that undergoes slow dissociation as a prerequisite for binding to vesicles, but this possibility was not investigated further. The burst of activity seen in the first few minutes may be due to the presence of a small amount of nonaggregated Pa2, which immediately binds to DMPM.

The initial velocity per enzyme for Pa2 acting on DMPM vesicles in the presence of PxB is 13 s^{-1}, about 6-fold lower than that for WT bvPLA2 (Table 1). The specific activity of Pa2 using the soluble substrate diC_6thio-PC is 5-fold lower than that of WT bvPLA2 under identical conditions (Table 1). Thus, it is likely that the somewhat low turnover of Pa2 on DMPM vesicles compared to bvPLA2 is due to the intrinsically lower specific activity of this enzyme compared to WT bvPLA2 and not due to a substantial decrease in the amount of Pa2 bound to anionic vesicles.

DISCUSSION

The main conclusion of the present study is that substitution of the six cationic lysine and arginine residues (14, 23, 58, 85, 94, and 133) on or near the putative i-face of bvPLA2 (Figure 1) to glutamates does not noticeably affect interfacial catalysis on anionic vesicles, although charge reversal mutagenesis does cause a modest reduction in affinity of enzymes for anionic vesicles. Although most of the data was obtained with phosphatidylmethanol vesicles, it was also found that E5 operates in the scooting mode on vesicles of the anionic phospholipid 1-palmitoyl-2-oleoylphosphatidylserine (not shown). On a very specific level, studies with these mutants establish K94 as the site for catalytically debilitating covalent modification by manoalogue and 12-*epi*-scalaradial. On a general level, these results also provide

a rationale for the fact that Pa2, with only one cationic residue on its putative i-face (Figure 1), is also highly catalytically functional on anionic vesicles. However, as developed below, the implications of the observations obtained with the charge reversal mutants of bvPLA2 are far-reaching in the context of interfacial recognition by PLA2s, a case study for lipid−protein interactions.

β-Loop of bvPLA2. The mutant in which the large β-loop of bvPLA2 has been deleted (Δ99−118) displays kinetic and vesicle binding properties virtually identical to those of WT. All secreted PLA2s have this β-loop, but its function has not been identified. Clearly, in the case of bvPLA2, the β-loop does not play a significant role in interfacial binding and catalysis on anionic interfaces.

Electrostatic versus Hydrophobic/Hydrogen-Bonding Interfacial Binding. Some of the factors underlying binding of PLA2 to the interface are elaborated below in terms of the hypothesis that the binding involves a large number of residues on a well-defined i-face. Such interactions along the i-face may involve an area of several hundred square angstroms, which may become inaccessible to the bulk aqueous phase and possibly desolvated (*45*). It has been estimated that values of K_d for most secreted PLA2s on anionic vesicles are $<10^{-12}$ M (*23*, *45*), and thus the overall interfacial binding energy over the i-face is >15 kcal/mol. Results presented here affirm that tight binding of PLA2 to anionic interfaces must come from multiple weak interactions; however, the task is to identify the factors that contribute toward these interactions. On the basis of the results at hand, it appears that hydrophobic (*46*−*48*), electrostatic (*15*, *19*, *49*, *50*), and hydrogen-bonding (*51*) interactions are implicated (*16*, *17*). The task of dissecting such contributions is daunting because they are interdependent (one may contribute to the other). As developed below, a limit estimate of the magnitude of electrostatic contributions for bvPLA2 interfacial binding can be judged from the results described in this paper.

Results with charge reversal mutants establish an upper limit estimate for K_d of 1 μM for all proteins (Figure 3). Intervesicle exchange studies show that multisite charge reversal mutants dissociate modestly faster than WT from anionic vesicles (Figure 5), but the shift does not raise K_d into the measurable range. If all of the observed increase in intervesicle exchange rate contributes toward K_d, then the results suggest that the 3−5 i-face basic residues together contribute a modest 2−3 kcal/mol to the interfacial binding energy of ≥15 kcal/mol.

A modest contribution of electrostatic interactions is supported by the HPLC experiments. The fact that acetonitrile is needed to elute bvPLA2 as well as other secreted PLA2s (unpublished observations and ref *44*) from the ester-IAM HPLC column suggests contributions to interfacial binding from hydrophobic and/or hydrogen-bonding interactions. One way to conceptualize the problem of interfacial binding of bvPLA2 is to imagine that the binding occurs along a surface that must come in close contact with the interface. The initial binding may depend in a distance-dependent manner on the electrostatic interactions, which may be significant at distances of 4−8 Å and are generally weak. On the other hand, significantly stronger hydrogen-bonding interactions between protein residues and phospholipid headgroups and glycerol diester backbones would require contacts in the 3−4 Å range. It is possible that the lack of binding of WT to the alkyl-IAM column, even in the absence of CH_3CN and NaCl, is due to the lack of enzyme−glycerol diester hydrogen bonding. The glycerol diester residues of the ester-IAM column may engage in hydrogen-bonding interactions with bvPLA2, accompanied by the hydrophobic effect. If this hydrophobic effect is due to penetration of i-face hydrophobic residues (Figure 1) into the hydrophobic interior of the bilayer, bvPLA2 should have bound to the ether-IAM column. Instead, the existence of numerous i-face hydrophobic residues close to the headgroup region of the bilayer may increase hydrogen bonding to the ester-IAM column since the hydrophobic, perhaps desolvated, microenvironment would destabilize hydrogen-bond donors and acceptors that are not paired with each other.

This hydrogen bonding promoted by the hydrophobic effect should be weakened in the presence of CH_3CN and would explain the observation that increasing CH_3CN in the mobile phase in the 0−45% range decreases the bvPLA2 elution time (Figure 7A). The fact that the elution time increases as CH_3CN is increased in the 45−55% range suggests that interfacial binding is not mainly due to the "classical" hydrophobic effect of inserting hydrophobic residues into the bilayer interior since the latter interaction decreases continuously as the percent CH_3CN increases. Perhaps at high CH_3CN, the hydrophobic i-face residues prefer to be in contact with bulk solvent, and the high free energy of bulk water in the low-polarity solvent increases bonding of water to the hydrogen-bonding donors and acceptors present on the i-face and at the bilayer interface. Clearly the biphasic response in Figure 7A shows that multiple factors are at work, and it is also possible that high CH_3CN causes gross structural changes in bvPLA2 that affect ester-IAM binding.

The fact that NaCl is also needed for elution from the ester-IAM column (Figure 7B) shows that electrostatic effects are at work as well, and this probably accounts for the shorter elution times of the multisite charge reversal mutants (Table 1). Charge reversal mutation decreases the retention time by up to 1.8-fold, but it is difficult to cast this in energetic terms. The proposed hydrophobic-promoted hydrogen bonding may be the main force driving the binding of Pa2 to vesicles where electrostatic binding is not likely with only one basic residue on the i-face (Figure 1). This enzyme, like bvPLA2, contains several i-face hydrophobic residues. As shown in Figure 1, bvPLA2 contains two histidines on its putative i-face (H11 and H56). These may be protonated and contribute to electrostatic interfacial binding; however, Pa2 does not have histidines on its putative i-face. Preliminary studies have shown that mutation of H11 and H56 of bvPLA2 to glutamate does not change the retention time for elution from the ester-IAM column. H11E and H56E also behave like WT in terms of scooting kinetics (Figure 2), binding to anionic vesicles (Figure 3), and intervesicle exchange (Figure 5).

Using a novel spin relaxation technique, we have been able to determine with high accuracy the orientation of bvPLA2 with respect to the membrane plane (*52*). In Figure 1, bvPLA2 is oriented so its i-face is parallel to the membrane plane. Clearly, the i-face contains numerous hydrophobic residues but contains only one of the basic residues (K14). It may be noted that of all the single site mutants, K14E

showed the weakest binding to the ester-IAM HPLC column (Table 1). Thus, the spin relaxation structural study suggests that the basic residues do not drive interfacial binding because they are not in close contact with the interface. This study also shows that bvPLA2 does not penetrate significantly into the membrane.

Mutagenesis studies are in progress to explore the role of surface hydrophobic residues of bvPLA2 in supporting interfacial binding. In this context, mutation of i-face residue L31 of porcine pancreatic PLA2 to polar residues results in a 10- to >17-fold decrease in apparent binding to micelles of hexadecylphosphorylcholine (*46*). Mutation of tryptophan 3 to alanine causes this enzyme to hop rather than scoot on DMPM vesicles (*47*). Clearly, this tryptophan is important for interfacial binding. Furthermore, this residue becomes shielded from bulk solvent water upon enzyme−vesicle contact (*45*). It is interesting to note that hydrophobic residues including tryptophan are important on the cellulose binding domain of cellulases for anchoring these enzymes to the "hydrophilic" surface of cellulose (*53*).

Recent studies with human group IIa secreted PLA2 have shown that mutation of the three basic residues on the putative i-face (R7, K10, and K16) to glutamates reduces binding to anionic vesicles by about 300-fold (*50*). These three residues contribute about 3 kcal/mol binding energy. Thus for this PLA2, i-face basic residues are more important for binding to anionic vesicles than they are for bvPLA2.

Binding of many secreted PLA2s, including bvPLA2, to zwitterionic phosphatidylcholine vesicles is weak (K_d > 1 μM) (*19*, *36*, *54*). It is now clear that preferential binding of bvPLA2 to anionic vesicles is not only due to electrostatics. The fact that addition of anionic fatty acid to phosphatidylcholine vesicles does not significantly increase interfacial binding of porcine pancreatic PLA2 (*55*) again supports that idea that electrostatic interfacial binding is not the dominant force. Presumably the fatty acid anion in a phosphatidylcholine vesicle does not provide the same interfacial environment that is found in DMPM vesicles for supporting tight enzyme binding.

McLaughlin and co-workers found that the *src* kinase-derived N-terminal peptide with an overall charge of +5 and without the myristoyl group binds to anionic vesicles of phosphatidylcholine/phosphatidylglycerol (2/1) with a K_d of 1 μM (binding energy of 4 kcal/mol), and this is predicted by Poisson−Boltzmann electrostatic calculations (*57*). Although it is difficult to extrapolate this result to the case of six basic residues on the i-face of bvPLA2, the estimate of a modest 2−3 kcal/mol for electrostatic interfacial binding of bvPLA2 to anionic vesicles is supported by expectations from Coulomb's law.

Anomalous Effects of NaCl and Interfacial Crowding of bvPLA2 Mutants. Compared to WT, R23E/K85E/K133E, K85E/K94E/K133E, and E5 are much more sensitive to salt-induced intervesicle exchange (Figures 4−6). The fact that the reduction in energy transfer of the mutants bound to DTPM vesicles clearly plateaus with >300 mM NaCl proves that complete dissociation of mutants into the aqueous phase does not occur. The observation of distinct fluorescence spectra for DTPM/dansyl-DHPE vesicles alone, enzyme-coated vesicles, and enzyme-coated vesicles in the presence of NaCl suggests that NaCl causes a transition between two or more vesicle-bound E* states rather than causing partial desorption of enzyme into the aqueous phase. Such residual binding, if it is due to hydrophobic and hydrogen-bonding interactions, is expected to be insensitive to changes in salt in the 0−0.4 M range used in this study. Our hypothesis is that multiple E* states exist, and i-face lysines and arginines work together to hold the enzyme in a more defined, intimate association with the interface.

The dansyl emission spectra of bvPLA2-coated anionic vesicles suggests that the probe becomes more exposed to bulk solvent water when NaCl is added, and this is more pronounced for the multisite mutants, especially R23E/K85E/K133E, compared to WT (Figure 8). One interpretation of these results is that the multisite charge reversal mutants sit on vesicles in a more "loosened" state in the presence of NaCl. This is consistent with the observation that the multisite mutants are more sensitive than WT to NaCl-induced intervesicle exchange (Figure 5). However, the fluorescence spectra under conditions of crowding of enzyme on vesicles must be viewed with caution. The fact that the efficiency of energy transfer is significantly lower for some of the multisite mutants under conditions of crowding but not at higher lipid/protein ratios (Figure 3B) is a reason for concern. Multiple factors may contribute to this, including nonideal mixing of fluorescent probe in enzyme-covered vesicles, and these are discussed in Supporting Information. The fluorescence studies under crowded conditions lead to the conclusion that NaCl does not cause interfacial desorption of enzyme, which again underscores the lack of strong electrostatic interfacial binding. However, these studies do not constitute proof for a "loosened" interaction between enzyme and interface. Whatever the effects of NaCl on the bound mutants are, it is clear that they have no consequence for interfacial catalysis because the turnover numbers for the multisite mutants acting on DMPM vesicles in the presence or absence of NaCl are similar to the turnover number of WT (Table 1).

These possible nonlinear energy transfer effects alluded to above cannot be the reason that the rate of intervesicle exchange starting with crowded enzyme on DTPM/dansyl-DHPE vesicles appears faster than under noncrowding conditions (Figure 9 versus Figure 5), since the nonlinear effect would give the appearance of slower intervesicle exchange (smaller decrease in energy transfer per unit time) under crowding versus noncrowding conditions. One hypothesis is that steric clashing of crowded bvPLA2s weakens interfacial binding, and this leads to "loosening" and faster intervesicle exchange, especially of the multisite mutants because they are anchored to the interface somewhat less tightly than is WT.

Inactivation of bvPLA2 by Manoalogue and 12-epi-Scalaradial. The results in this study showing that K94E is completely resistant to inactivation by manoalogue and 12-*epi*-scalaradial strongly suggest that modification of K94 by these natural products is responsible for loss of enzymatic activity. This site is consistent with peptide mapping (*30*) and modeling (*58*) studies. Thus, it can now be concluded that the major attachment site is responsible for inactivation. The presence of enzyme-bound manoalide may prevent the region of the i-face near K94 from tightly interacting with the interface, although manoalide modification does not prevent interfacial binding, and it leaves the active site functional for the hydrolysis of short-chain phospholipids

(*32*). Also, interfacial binding of manoalogue-modified bvPLA2 does not result in complete desolvation of the microenvironment between the interface and the enzyme (*32*). The manoalide/12-*epi*-scalaradial binding site on bvPLA2 proposed by Roggo et al. and supported by the present data would place manoalide on the putative i-face of bvPLA2 near the active-site slot but not covering it. The reduced catalytic efficiency of the modified enzyme bound to anionic vesicles (*32*) is consistent with the hypothesis that desolvation of the microinterface is important for interfacial catalysis.

Dennis and co-workers have shown that mutation of both K6 and K79 of cobra venom PLA2 to arginine is necessary and sufficient to make the enzyme completely resistant to inactivation by manoalide (*59*). These lysines lie on the putative i-face of cobra venom PLA2, and manoalide modification does not alter the activity of this enzyme on water-soluble substrates The fact that two lysines appear to be modified suggests that manoalide may not bind to a distinct site on cobra venom PLA2, which may explain why this natural product is a less potent inactivator of the snake venom enzyme compared to bvPLA2. It is not clear whether inactivation of cobra venom PLA2 by manoalide is due to decreased membrane binding or to catalytically nonproductive interfacial binding.

ACKNOWLEDGMENT

We are grateful for Dr. David L. Scott for constructing the homology model of Pa2, to Thomas Dudler for preparing Δ99−118 DNA, and to Eric Swanson and Professor T. Lybrand for help in generating Figure 1 and in the use of the Delphi program.

SUPPORTING INFORMATION AVAILABLE

Experimental details of mutagenesis and fluorescence spectra and four figures, showing inactivation of bvPLA2s by manoalogue and 12-*epi*-scalaradial, Ca^{2+} binding to E*, tryptophan emission spectra, and dansyl emission difference spectra via resonance energy transfer (13 pages). Ordering information is given on any current masthead page.

REFERENCES

1. Sambrook, J., Fritsch, E. F., & Maniatis, T. (1989) *Molecular Cloning*: *A Laboratory Manual*, Cold Spring Harbor Laboratory Press, Cold Spring Harbor, NY.
2. Dudler, T., Chen, W.-Q., Wang, S., Schneider, T., Annand, R. R., Dempcy, R. O., Crameri, R., Gmachl, M., Suter, M., & Gelb, M. H. (1992) *Biochim. Biophys. Acta 1165*, 201−210.
3. Lin, H.-K., & Gelb, M. H. (1993) *J. Am. Chem. Soc. 115*, 3932−3942.
4. Verheij, H. M., Slotboom, A. J., & De Haas, G. H. (1981) *Rev. Physiol. Biochem. Pharmacol. 91*, 91−203.
5. Waite, M. (1987) *The Phospholipases*, Plenum, New York.
6. Dennis, E. A. (1997) *Trends Biochem. Sci. 22*, 1−2.
7. Verger, R., & de Haas, G. H. (1976) *Annu. Rev. Biophys. Bioeng. 5*, 77−117.
8. Dennis, E. A. (1983) *Enzymes 16*, 307−353.
9. Jain, M. K., Gelb, M. H., Rogers, J., & Berg, O. G. (1995) *Methods Enzymol. 249*, 567−614.
10. Jain, M. K., & Berg, O. (1989) *Biochim. Biophys. Acta 1002*, 127−156.
11. Gelb, M. H., Jain, M. K., Hanel, A. M., & Berg, O. (1995) *Annu. Rev. Biochem. 64*, 653−688.
12. Thunnissen, M. M. G. M., Ab, E., Kalk, K. H., Drenth, J., Dijkstra, B. W., Kuipers, O. P., Dijkman, R., De Haas, G. H., & Verheij, H. M. (1990) *Nature 347*, 689−691.
13. Scott, D. L., White, S. P., Otwinowski, Z., Yuan, W., Gelb, M. H., & Sigler, P. B. (1990) *Science 250*, 1541−1546.
14. Yu, B.-Z., Berg, O. G., & Jain, M. K. (1993) *Biochemistry 32*, 6485−6492.
15. Han, S. K., Yoon, E. T., Scott, D. L., Sigler, P. B., & Cho, W. (1997) *J. Biol. Chem. 272*, 3573−3582.
16. Dijkstra, B. W., Renetseder, R., Kalk, K. H., Hol, W. G., & Drenth, J. (1983) *J. Mol. Biol. 168*, 163−179.
17. Ramirez, F., & Jain, M. K. (1991) *Proteins*: *Struct., Funct., Genet. 9*, 229−239.
18. Scott, D. L., & Sigler, P. B. (1994) *Adv. Protein Chem. 45*, 53−88.
19. Jain, M. K., Egmond, M. R., Verheij, H. M., Apitz-Castro, R., Dijkman, R., & De Haas, G. H. (1982) *Biochim. Biophys. Acta 688*, 341−348.
20. Volwerk, J. J., Jost, P. C., de Haas, G. H., & Griffith, O. H. (1986) *Biochemistry 25*, 1726−1733.
21. Pluckthun, A., & Dennis, E. A. (1985) *J. Biol. Chem. 260*, 11099−11106.
22. Jain, M. K., Rogers, J., Jahagirdar, D. V., Marecek, J. F., & Ramirez, F. (1986) *Biochim. Biophys. Acta 860*, 435−447.
23. Jain, M. K., Ranadive, G., Yu, B.-Z., & Verheij, H. M. (1991) *Biochemistry 30*, 7330−7340.
24. Jain, M. K., Maliwal, B. P., De Haas, G. H., & Slotboom, A. J. (1986) *Biochim. Biophys. Acta 860*, 448−461.
25. Gomez, F., Vandermeers, A., Vandermeers-Piret, M.-C., Herzog, R., Rathe, J., Stievenart, M., Winand, J., & Christophe, J. (1989) *Eur. J. Biochem. 186*, 23−33.
26. Glaser, K. B., & Jacobs, R. S. (1986) *Biochem. Pharmacol. 35*, 441−453.
27. Lombardo, D., & Dennis, E. A. (1985) *J. Biol. Chem. 260*, 7234.
28. Glaser, K. B., Carvalho, M. S. D., Jacobs, R. S., Kernan, M. R., & Faulkner, D. J. (1989) *Mol. Pharmacol. 36*, 782−788.
29. de Carvalho, M. S., & Jacobs, R. S. (1991) *Biochem. Pharmacol. 42*, 1621−1626.
30. Glaser, K. B., Veduick, T. S., & Jacobs, R. S. (1988) *Biochem. Pharmacol. 37*, 3639−3646.
31. Reynolds, L. J., Mihelich, E. D., & Dennis, E. A. (1991) *J. Biol. Chem. 266*, 16512−16517.
32. Ghomashchi, F., Yu, B. Z., Jain, M. K., & Gelb, M. H. (1991) *Biochemistry 30*, 9559−9569.
33. Yuan, W., Quinn, D. M., Sigler, P. B., & Gelb, M. H. (1990) *Biochemistry 29*, 6082−6094.
34. Annand, R. R., Kontoyianni, M., Penzotti, J. E., Dudler, T., Lybrand, T. P., & Gelb, M. H. (1996) *Biochemistry 35*, 4591−4601.
35. Jain, M. K., & Gelb, M. H. (1991) *Methods Enzymol. 197*, 112−125.
36. Yu, B.-Z., Ghomashchi, F., Cajal, Y., Annand, R. A., Berg, O. G., Gelb, M. H., & Jain, M. H. (1997) *Biochemistry 36*, 3870−3881.
37. Rogers, J., Yu, B. Z., & Jain, M. K. (1992) *Biochemistry 31*, 6056−6062.
38. Berg, O. G., Yu, B.-Z., Rogers, J., & Jain, M. K. (1991) *Biochemistry 30*, 7283−7297.
39. Jain, M. K., Rogers, J., Berg, O., & Gelb, M. H. (1991) *Biochemistry 30*, 7340−7348.
40. Cajal, Y., Berg, O. G., & Jain, M. K. (1995) *Biochem. Biophys. Res. Commun. 210*, 746−752.
41. Cajal, Y., Rogers, J., Berg, O. G., & Jain, M. K. (1996) *Biochemistry 35*, 299−308.
42. Jain, M. K., De Haas, G. H., Marecek, J. F., & Ramirez, F. (1986) *Biochim. Biophys. Acta 860*, 475−483.
43. Fairbank, R. W. P., & Wirth, M. J. (1997) *Anal. Chem. 69*, 2258−2261.
44. Ong, S., Liu, H., & Pidgeon, C. (1996) *J. Chromatogr. A 728*, 113−128.
45. Jain, M. K., & Vaz, W. L. C. (1987) *Biochim. Biophys. Acta 905*, 1−8.

46. Kuipers, O. P., Kerver, J., van Meersbergen, J., Vis, R., Dijkman, R., Verheij, H. M., & De Haas, G. H. (1990) *Protein Eng. 3*, 599−603.
47. Liu, X., Zhu, H., Huang, B., Rogers, J., Yu, B. Z., Kumar, A., Jain, M. K., Sundaralingam, M., & Tsai, M. D. (1995) *Biochemistry 34*, 7322−34.
48. Lee, B.-I., Yoon, E. T., & Cho, W. (1996) *Biochemistry 35*, 4231−4240.
49. Dua, R., Wu, S.-K., & Cho, W. (1995) *J. Biol. Chem. 270*, 263−268.
50. Snitko, Y., Koduri, R. S., Han, S. K., Molini, B., Wilton, D. C., Gelb, M. H., & Cho, W. (1998) *Biochemistry* (in press).
51. Zhou, F., & Schulten, K. (1996) *Proteins*: *Struct., Funct., Genet. 25*, 12−27.
52. Lin, Y., Nielsen, R., Murray, D., Mailer, C., Hubbell, W. L., Robinson, B. H., & Gelb, M. H. (1998) *Science 279*, 1925−1929.
53. Din, N., Forsythe, I. J., Burtnick, L. D., Gilkes, N. R., Miller, R. C. Jr., Warren, R. A. Kilburn, D. G. (1994) *Mol. Microbiol. 11*, 747−755.
54. Bayburt, T., Yu, B. Z., Lin, H. K., Browning, J., Jain, M. K., & Gelb, M. H. (1993) *Biochemistry 32*, 573−582.
55. Jain, M. K., & De Haas, G. H. (1983) *Biochim. Biophys. Acta 736*, 157−162.
56. Buser, C. A., Sigal, C. T., Resh, M. D., & McLaughlin, S. (1994) *Biochemistry 33*, 13093−13101.
57. Ben, T. N., Honig, B., Peitzsch, R. M., Denisov, G., & McLaughlin, S. (1996) *Biophys. J. 71*, 561−575.
58. Ortiz, A. R., Pisabarro, M. T., & Gago, F. (1993) *J. Med. Chem. 36*, 1866−79.
59. Bianco, I. D., Kelley, M. J., Crowl, R. M., & Dennis, E. A. (1995) *Biochim. Biophys. Acta 1250*, 197−203.
60. Scott, D. L., Otwinowski, Z., Gelb, M. H., & Sigler, P. B. (1990) *Science 250*, 1563−1566.

BI972525I